DOI: https://doi.org/10.54966/jreen.v1i1.1467

Journal of Renewable Energies

Revue des Energies Renouvelables

Journal home page: https://revue.cder.dz/index.php/rer

Conference paper

Comparative Numerical Study on Nanofluid-Based Cooling Strategies in PVT Systems for Improved Thermodynamic and Electrical Performance

Mrinmoy Roy Rony [a,*], **Shihab Shahriare** [a], **Abdullah All Motacabbir** [a], **Chandrmani Yadav** [b]

[a] *Department of Mechanical Engineering, Chittagong University of Engineering and Technology, Chattogram-4349, Bangladesh*

[b] *Marwadi University Research Centre, Faculty of Engineering & Technology, Department of Mechanical Engineering, Marwadi University, Rajkot, 360003, Gujarat, India*

ARTICLE INFO

Article history:
Received: December 11, 2024
Accepted: July 15, 2025
Available online July 23, 2025
Published: July 24, 2025

Keywords:
PVT,
Nanofluid,
Thermal Performance,
Electrical Efficiency,
CFD.

ABSTRACT

The study presents an optimization technique to improve photovoltaic-thermal module's performance by analyzing cooling effects facilitated by mono and hybrid nanofluids. The investigation evaluates the thermal performance of silver-water (Ag/water), aluminum oxide-water (Al2O3/water), and hybrid combinations of magnesium oxide and copper oxide with multi-walled carbon nanotube-water (MgO-MWCNT/water and CuO-MWCNT/water) nanofluids. The prototype model integrates four riser tubes and an absorber plate to facilitate heat transfer mechanisms. A novel approach is employed wherein each consecutive tube's inlet is rotated by 180° to ensure uniform heat distribution across the solar panel absorber. Numerical simulations using computational fluid dynamics were conducted in ANSYS Fluent to assess the cooling effects of circulating nanofluids throughout the absorber plate. Results indicate that optimal electrical efficiency enhancements are achieved at a fluid velocity of 0.24 m/s with Al2O3/water at 10.7%, Ag/water at 10.78%, MgO-MWCNT/water at 10.69%, and CuO-MWCNT/water at 10.68%. The exergy efficiency values for the nanofluids, at the same flow rate, are 11.8% for Al2O3/water, 12.2% for Ag/water, 11.2% for MgO-MWCNT/water, and 11.4% for CuO-MWCNT/water. The results demonstrate the superior thermal and electrical performance of Ag/water, suggesting its viability for improving photovoltaic efficiency and supporting sustainable energy production.

* *Corresponding author, E-mail address: mrinmoyroyrony3@gmail.com*
Tel : +8801609531477

ISSN: 1112-2242 / EISSN: 2716-8247

1. INTRODUCTION

Global energy consumption is steadily increasing while conventional fossil fuel sources continue to decline rapidly. This shift has led to growing interest in alternative and renewable energy solutions. Environmentally friendly energy resources offer a high level of environmental safety, and among them, solar energy is the prominent and widely applicable. Researchers are actively working to improve the efficiency and usability of solar energy systems.

Solar panels are the most effective means of harnessing sunlight. Photovoltaic cells are a simple medium to harvest sunlight, available year-round. Photon energy from sunlight appears in two forms: heat and light. While both are convertible, excess heat reduces solar cell efficiency. Direct exposure to sunlight increases the temperature of panels, significantly decreasing their electrical efficiency. Any increase in temperature beyond the rated 25°C reduces the solar panel's output power by 0.4-0.5% per degree (Ebaid et al., 2018). Appropriate cooling can prolong the life of solar panels, lower cell disintegration, and increase electricity production. In this regard, the circulation of cooling liquid through a heat exchanger in direct thermal connection with the rear side of the solar photovoltaic module is the best solution. Technological fluids can now have better thermal, rheological, and tribological properties by using a novel type of cooling liquid called nanofluids. For instance, when single nanoparticles are dispersed in water (base fluid), the resulting mixture is called mono-nanofluid. Another type combines metallic and metal oxide particles, forming hybrid nanofluids known for their improved thermal conductivity, chemical inertness, and stability (Huminic & Huminic, 2020). Metallic nanoparticles (like Ag, Cu, and Au) exhibit greater thermal conductivity but lower chemical stability compared to metal oxide particles (like Al_2O_3 and CuO), which are more stable but possess lower thermal conductivity.

Regarding photovoltaic thermal collectors, numerous studies have been carried out. Selmi et al. (2008) utilized CFD tools to numerically analyze the performance of a flat plate solar thermal collector operating with water flow. It analyzed water circulation, heat transfer mechanisms, and solar radiation. A close correlation was observed between the simulated results and experimental findings. Usama Siddiqui et al. (2012) devised an experimental setup similar to Selmi et al. (2008), presenting a 3-dimensional numerical model. A thermal prototype was developed to examine the heat transmission of the PV modules under both cooled and uncooled conditions. The module was used to compute the electricity production of the panels in conjunction with an electrical and radiation model. According to the findings, panel performance with cooling had little effect on radiation that was absorbed, whereas panel performance significantly declined without cooling. A study on the temperature changes of a water-cooled PV solar setup is discussed by Kozak et al. (2009). They used a mathematical module for the heat exchanger and analyzed how the plate temperature varied with the amount of cooling water under different power levels and inlet water temperatures. These results showed that overall efficiency was 14% lower for theoretical panels and 30% lower for actual panels. Khanjari et al. (2016) performed a CFD analysis on a PVT setup utilizing nanofluid/water. The study showed that nanofluids based on alumina/water and Ag/water increased heat transfer coefficients by 12% and 43%, respectively, depending on the volume fraction. Tian et al. (2021) studied the impact of nanofluid to cool a solar/thermal panel using energy and exergy analysis. According to the study findings, incorporating 1% nanoparticles at a volume flow rate of 0.5 L/min improves exergy efficiency by 0.45%. Davarnejad and Jamshidzadeh (2015) investigated MgO-water nanofluid heat transfer attributes under turbulent flow using CFD modeling. They observed that elevating the volume fraction of the nanofluid resulted in an increase in the Nusselt Number. To decrease the temperature of the solar/thermal panel and boost photovoltaic electricity production, Sathyamurthy et al. (2021) assessed CNT/Alumina nanoparticles in a solar panel. Due to the application of these nanocoolants, the PVT module had significant heat removal

from the collector, resulting in power increases of 11.7% and 21.4%, respectively, in comparison to a standalone PV module. In an experiment, Murtadha and Hussein (2022) optimized the performance of solar panels by utilizing a one-pass flow system and various concentrations of Al_2O_3 nanofluid acting as a coolant. In the study, using nanofluid at a 3-weight percent concentration resulted in the most significant improvement in power generation. A 13% increase in Panel power was observed when this nanofluid concentration was applied for cooling. Hussien et al. (2014) studied the utilization of Al_2O_3/water nanofluid coolant to improve solar panel performance. When tested under typical experimental conditions (1000 W/m^2 radiation and a 24-hour evaluation period), employing nanofluid at 0.3% concentration with a constant flow of 0.2 L/s resulted in a decreased temperature of 42.2 °C. This adjustment contributed to an enhancement in the solar panel's efficiency to 12.1%. Hamdan and Kardasi (2017) conducted an investigation where three identical photovoltaic modules were positioned adjacent for cooling effect observation. Two of these panels were subjected to cooling using pure water and nanofluids, while the third panel served as to control. Different concentrations of Al_2O_3 and CuO nanoparticles were combined with distilled water to form the nanofluid, and the optimal concentration for each was determined. The results of the study revealed that adding 0.4% weight percentage of Al_2O_3 to pure water raised solar panel conversion performance by 2%. Similarly, the inclusion of 0.6% CuO resulted in a 2.34% efficiency increase. In a separate investigation, Xu and Kleinstreuer (2014) developed a solar cogeneration technique incorporating nanofluids for both heating and cooling purposes. Also, maintaining the nanofluid outlet at approximately 62 °C allowed the system to achieve 70% overall efficiency. The electrical and thermal components would contribute 11% and 59%, respectively. In essence, the study concluded that a nanofluid-based system offers long-term superiority over a water-based system. Ibrahim et al. (2023) examined how Al_2O_3 affected the heat transfer and electrical output of polycrystalline photovoltaic modules in outdoor settings. The study revealed a 15.5% improvement in PVT electrical conversion efficiency. With Al_2O_3 added at 0.05% volume and a fluid flow of 0.07 kg/s, the PVT module's surface temperature dropped by 22.83% relative to the baseline panel. At peak solar intensity, the uncooled PVT unit reached 75.5 °C and about 12.16% electrical efficiency. Cooling with water and nanofluids lowered the temperature by 10 °C and 20 °C, respectively.

Only a few computational studies have used high thermal conductivity nanofluids to increase heat transfer. To address this gap, the present study investigates a PVT configuration featuring an absorber plate integrated with four rear riser tubes, through which four different nanofluids are circulated to provide thermal cooling. The numerical analysis is conducted using CFD simulation in ANSYS Fluent to analyze several nanofluids cooling effects in a Photovoltaic module. The nanofluids include 5% volume concentration of Al_2O_3/water, and Ag/water, as well as 80% MgO combined with 20% MWCNT / water at 2% volume concentration and 50 ℃, and similarly 80% CuO with 20% MWCNT / water under identical conditions. The system is designed with each consecutive inlet flow reversed by 180 degrees to achieve uniform thermal distribution.

The objective of this study is to numerically examine the effects of several types of nanofluids on the thermal and electrical efficiencies of the PVT system. The study uses ANSYS Fluent to model the cooling performance of four types of nanofluids under different flow inlet velocities. So, the aim is to improve the energy yield, evaluate the exergy and heat transfer aspect, and find out the most economical and efficient cooling schemes for the PV modules. The effects of nanofluid quality and inflow velocity are also investigated to enhance the system performance at standard test conditions.

2. NUMERICAL MODELING AND METHODOLOGY

This section discusses the methodology utilized for computational simulation of the photovoltaic/thermal configuration using nanofluids. Figure (1) illustrates the procedural flowchart adopted in the present study.

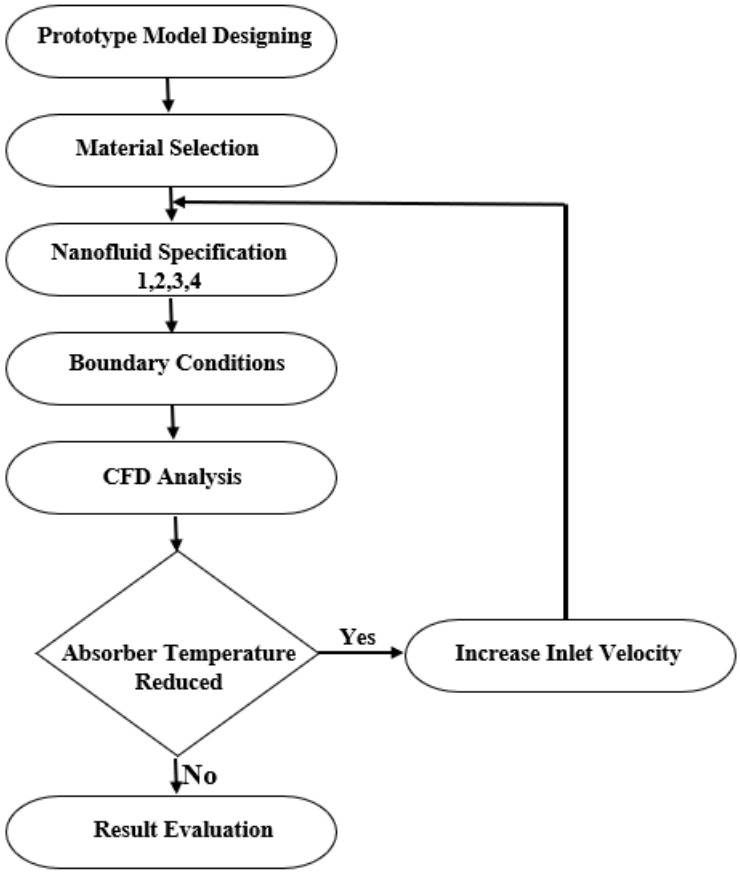

Fig 1. Flowchart depicting the methodology employed in the analysis phase of the research

2.1 Model Geometry

The modeling process began with the geometry shown in Fig. (2). The proposed PVT included a covered glass, a solar panel, a heat-conducting layer, and flow conduits called a header and riser. Four identical riser tubes were used, with alternating inlet and outlet directions. Each subsequent tube was rotated 180° relative to the previous one. The geometry was modeled by SOLIDWORKS. Table 1 presents the geometric parameters of the model. Boundary conditions were used to represent the effects of the PV panel and front glass, while detailed geometric modeling was carried out for the absorber plate and riser tubes. Additionally, the absorptivity of the solar panel, the material utilized for the plate, and the transmittance of the aperture area influenced the energy absorbed by the plate under solar radiation. The dimensions and panel characteristics were taken from (Khanjari et al., 2016).

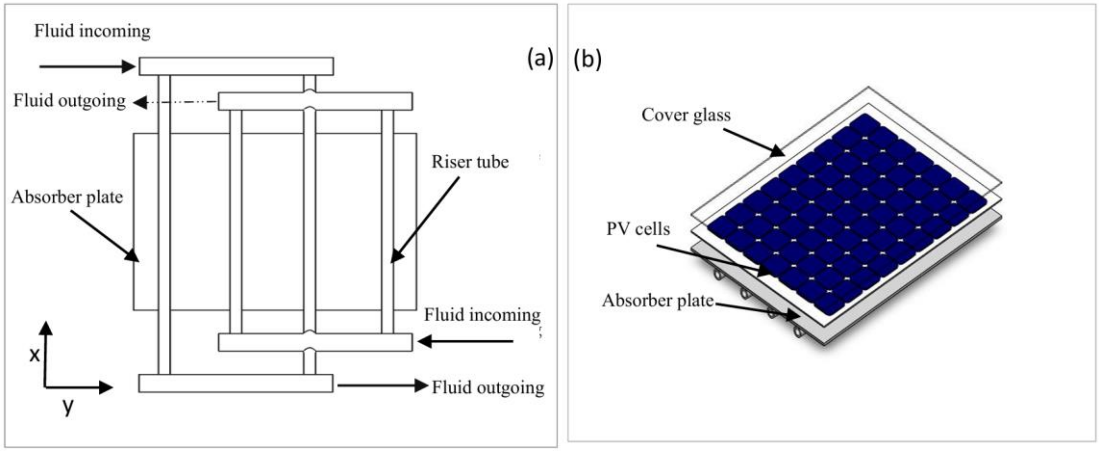

Fig 2. Configuration of the developed PVT setup (a), Illustration depicting the configuration and its elements(b)

Table 1. Specifications, features, and contents for the different components of the prototype design

Riser tubes	Total riser tubes: 4 Length: 1 m Outward diameter: 10 mm tube thickness: 1 mm The riser center spacing: 500 mm Material: Copper $\rho = 8978 \text{kg} m^{-3}$; $k = 387.6 W/m\ K$; $C_P =$ 381 J/kg K
Plate-Absorber	Length: 2000 mm Width: 1000 mm Thickness: 6 (m) Material: Copper
Headers	Total number of headers: 4 Outer diameter: 2 mm tube thickness: 1 mm Material: Copper $\rho = 8978 \text{kg} m^{-3}$; $k = 387.6 W/m\ K$; $C_P =$ 381 J/kg K
PV module	Riser cells number: 60 Length: 1640 mm Width: 990 mm PV panel absorptance: 0.9 The emissivity of the solar panel: 0.88 $\beta_r = 0.0045 ℃^{-1}$ $\eta_r = 12\%$ at 0℃
Glass Emissivity	0.88
Set up tilt angle	35°

2.2 Meshing

Discretizing the governing equations is influenced by the flow characteristics, and the geometry typically involves control volumes or elements. To solve the discretized equations, the computational domain must be meshed accordingly. The PVT module comprises two distinct geometric regions, which are cylindrical geometries (tubes and fluid domain) and rectangular geometries (absorber plate and photovoltaic panel), each requiring an appropriate meshing technique for accurate CFD simulation. Standard three-dimensional meshing was done in the present study. Due to the thin geometry of the absorber plate, sweep meshing was applied. Tetrahedral elements for the fluid domain were generated using the Patch-conforming meshing technique for the domain's fluid body. Inflation layers were applied near the tube walls to resolve boundary layer effects. The final mesh consists of 4443976 nodes and 6549355 elements. The module's mesh structure is displayed in Fig. (3).

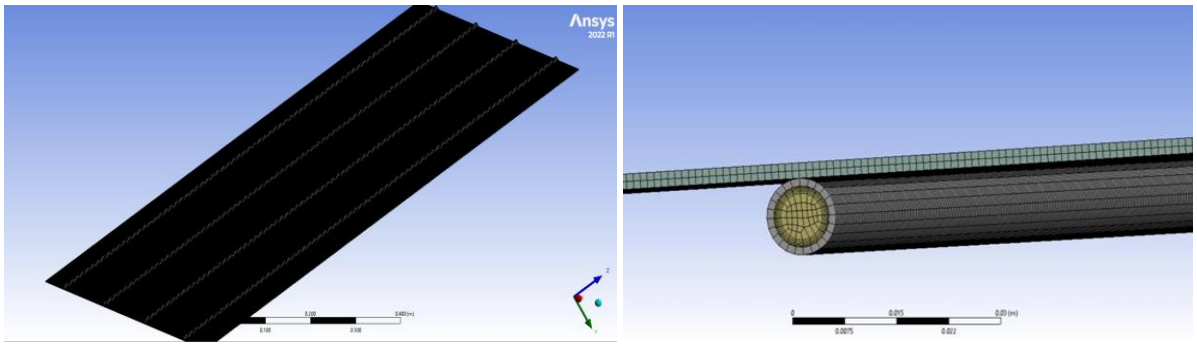

(a) Whole PVT system including 4 tubes (b) Amplified view of a single tube

Fig 3. The meshing of the photovoltaic thermal system

2.3 Working Fluid Features

Enhancing system efficiency requires a thorough analysis of operational fluids. The base fluid, water's thermo-physical properties, were characterized through temperature-based relationships sourced from the literature (Kell, 1975; Shang, 2012). The addition of nanoparticles altered the fluid's physical properties, depending upon factors such as concentration. Ideal nanofluids exhibit high thermal conductivity and low viscosity. Traditional conductivity models assume that nanoparticles remain stationary relative to the base liquid. Conversely, models based on dynamic conductivity account for the irregular motion of nanoparticles, which enhances thermal transport through micro-scale mixing (Khanjari et al., 2016). Based on insights from the literature review, we utilized four types of nanofluids, each optimized for specific aspect ratios to achieve the best performance. Table 2 lists the thermophysical properties of the selected nanofluids at a typical temperature. These properties were obtained from (Khanjari et al., 2016 ; Muneeshwaran et al., 2021).

Table 2. Thermo-physical characteristics of the nanofluids utilized in this research

Nanofluid specifications	φ %	k_{nf}	μ_{nf}	$C_{P_{nf}}$	ρ_{nf}
Ag/water	5	1.2461	0.000741	2768.2	1467.6
Al2O3/water	5	0.7613	0.000741	3585.1	1141.1
80% MgO - 20% MWCNT / water	2	0.7	0.00079	3674	1040
80%CuO - 20% MWCNT / water	2	0.71	0.00082	3785	1048

2.4 Boundary Conditions

The simulation study focused on evaluating working fluid performances across a range of inlet velocities. Since the flow was incompressible and the outlet pressure values were known, the pressure outlet condition was selected. The coupled condition was employed to model heat transmission across the fluid-solid contact regions. The simulation utilized solar irradiation as a constant heat flux (Corbin & Zhai, 2010). Two distinct heat transfer mechanisms were used: convection through the fluids in the tubes and conductive transfer linking the absorber plate to the risers. Table 3 lists the boundary conditions used, and Fig. (4) shows their respective application surfaces.

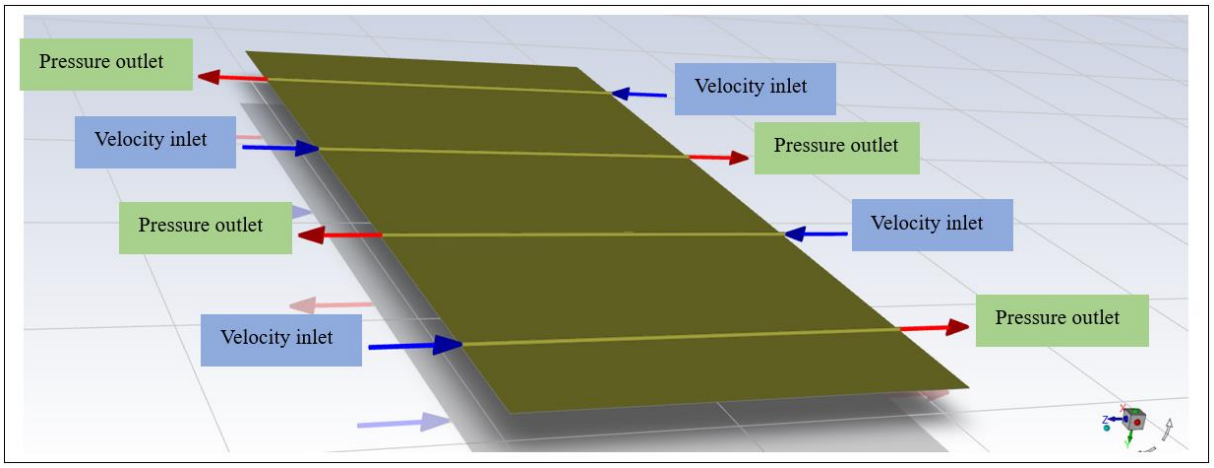

Fig 4. Proposed tube plate boundary conditions interface

Equation (7) was used to compute the absorbed solar radiation, accounting for PV power output, glass transmittance, and plate absorptivity. Adiabatic wall boundary conditions were maintained for both the tube's exterior and the backside of the plate. Conversely, the front surface of the plate was subjected to a uniform heat flux. An essential consideration is the influence of gravitational acceleration, which significantly impacts both buoyant force and convection effects. To incorporate gravity effects in the simulation, the tilt angle of the setup was activated. The definitions for the gravity acceleration vectors are outlined as

$$g_x = 0\ ;\ g_y = gcos\theta\ ;\ g_z = -gsin\theta.$$

Table 3. Details of boundary conditions applied in the analysis

Inlet conditions	Outlet conditions	Solid-liquid interface
v_x=v_y=0 m/s	P=1 atm (static pressure)	v_x=v_y=v_z= 0 m/s
v_z= (0.5 to 0.25) m/s		q = 570.24 W/m^2
T=T_{in}=298K		A_{coll}= 0.8
G_t= 800 W/mK^{-1}		$T_s = 5774K$

2.5 Governing Equations and Solver Conditions

In this study, the materials used in the photovoltaic thermal layer had temperature-independent thermophysical properties. A single-phase approach was employed, assuming thermal equilibrium between the base fluid and nanoparticles. The working fluid was considered Newtonian, steady, incompressible, and three-dimensional. Simulations were performed over a velocity range of 0.05 to

0.24 m/s, where the Reynolds number fell within the turbulent regime. Therefore, the SST k-*ω* turbulent model, developed by Menter (1993) and suitable for use in transition zones and at low Reynolds numbers (Saffarian et al., 2020), was employed. The continuity (mass), RANS momentum, and energy equations were resolved through the finite volume technique. Pressure-velocity coupling was managed using a pressure-based solver and the SIMPLE scheme. Second-order upwind discretization and the least squares gradients methods were applied. The simulation converged when the energy, velocity, and continuity residuals fell below 10^{-6}, 10^{-3}, and 10^{-4}, respectively.

2.6 Energy Analysis

According to the principle of energy conservation, energy transforms between different forms but is never lost. Within the PVT setup, sunlight is converted into thermal and electrical outputs. The thermal and electrical efficiency were calculated to evaluate system performance, combined to determine overall efficiency. Equations (9) to (11) were employed to calculate the electrical, thermal, and overall efficiency of the photovoltaic panel.

2.7 Exergy Analysis

Exergy is described as how much of a system's energy can be harnessed as work before reaching thermal equilibrium with its surroundings. Unlike energy, exergy is destroyed in real processes due to irreversibility. Exergy analysis helps identify and minimize irreversibilities to improve system efficiency. In PVT systems, exergy analysis evaluates both electrical and thermal outputs. Since the electrical output is already high-quality energy, its exergy is simple to calculate. The exergy of the thermal output depends on the heat source temperature and ambient conditions. During this investigation, the module's exergy values were derived using Eqs. (14) to (17).

2.8 Thermophysical and Performance Equations

The well-known Einstein equation, as presented by Drew and Passman (1999), provides a way to estimate the viscosity of nanofluids containing low volume concentrations (typically less than 5%). The equation is presented as follows.

$$\mu_{nanofluid} = (1 + 2.5\varphi)\,\mu_{water} \tag{1}$$

Here φ is the volumetric concentration of the nanoparticles, $\mu_{nanofluid}$ is the nanofluid viscosity (kg/ms), and μ_{water} is the water viscosity (*kg/ms*). Using this relation, the thermal conductivity of the nanofluids formulated by Yu and Choi (2003).

$$k_{nanofluid} = \frac{k_p + 2k_f - 2(k_f - k_p)\varphi}{k_p + 2k_f - (k_f - k_p)\varphi} K_f \tag{2}$$

Here k_f, and, k_p are the thermal conductivity (*W/m°c*) of the base liquid and nanoparticle, respectively. This relation is used to evaluate the nanofluid density (Hussein et al., 2017 ; Hussien et al., 2014).

$$\rho_{nanofluid} = (1 - \varphi)\rho_f + \varphi\rho_P \tag{3}$$

Here, the specific heat equation developed by Xuan and Roetzel (2000) is as follows :

$$(\rho C_P)_{nf} = (1-\varphi)(\rho C_P)_f + \varphi(\rho C_P)_P \tag{4}$$

$$\varphi = \frac{V_{NP}}{V_T} \tag{5}$$

Here, V_T is the whole volume (m^3), and V_{NP} is the nanoparticle volume (m^3). The above correlations produce the thermal diffusivity equation (Hussein et al., 2017) as :

$$\alpha_{nanofluid} = \frac{k_{nf}}{\rho_{nf} Cp_{nf}} \tag{6}$$

The heat flux absorbed on the plate is given by :

$$q = G_t T_g \alpha(1-\eta) \tag{7}$$

$$RMSE = \sqrt{(\frac{\sum Error^2}{n})} \tag{8}$$

$$\eta_e = \eta_r[1-\beta(T_c - T_r] \tag{9}$$

$$\eta_{th} = \frac{\dot{m} C_P (T_{out} - T_{in})}{G_t A_c} \tag{10}$$

$$\eta_{overall} = \eta_e + \eta_{th} \tag{11}$$

$$PEEI = \frac{\eta_{e(at\ v=0.24\ ms^{-1})} - \eta_{e(at\ v=0.04\ ms^{-1})}}{\eta_{e(at\ v=0.4\ ms^{-1})}} \times 100 \tag{12}$$

$$MPEEI = \frac{\eta_{e(at\ v=0.24\ ms^{-1}, nanofluid)} - \eta_{e(at\ v=0.24\ ms^{-1}, pure\ water)}}{\eta_{e(at\ v=0.04\ ms^{-1}, pure\ water)}} \times 100 \tag{13}$$

Typically, the equation for exergy balance forms the basis for identifying exergy dissipations using a positive balance method. For a typical PVT module, this equation (Wu et al., 2015) is stated in the following manner.

$$\dot{E}_{x_{thermal}} = \dot{m}_{fluid} C_{P_{fluid}} [T_{out} - T_{in}] - T_o ln(\frac{T_{out}}{T_{in}}) \tag{14}$$

$\dot{E}x_{thermal}$ is the thermal exergy derived from the coolant. Electric exergy is commonly used to describe the energy produced by a solar cell (Wu et al., 2015), as it signifies usable energy that can be fully harnessed for practical applications. Moreover, electrical energy remains unaffected by the environmental state. Electric exergy is typically associated with the cell power conversion efficiency, denoted by η_{cell}.

$$\dot{E}x_{photovoltaic} = \eta_{cell} S_t A_{coll} \tag{15}$$

The solar exergy $\dot{E}x_{solar}$ is calculated using the Petela equation (Wu et al., 2015), which accounts for ambient and solar temperatures.

$$\dot{E}x_{solar} = 0.95 S_t A_{coll} \tag{16}$$

From the second law of efficiency (Khanjari et al., 2016) :

$$\eta_{II} = \frac{\dot{E}x_{photovoltaic} + \dot{E}x_{thermal}}{\dot{E}x_{solar}} \tag{17}$$

3. RESULTS

3.1 Validation

The current study is validated with reference to the work of Khanjari et al. (2016). Utilizing the RMSE method of Eq. (8) for error prediction, the simulation study has a 5.4% error in electrical efficiency increase compared to the reference model, reflecting that there are quite reasonable values obtained from the simulation model in comparison to the reference paper.

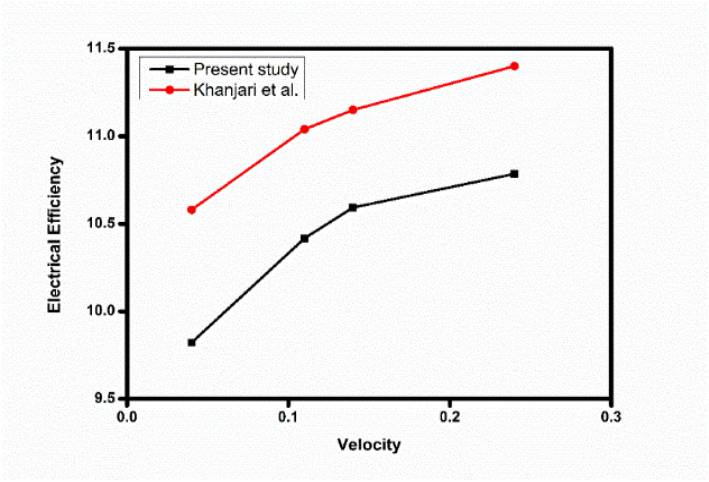

Fig 5. Electrical efficiency values compared with an experimental study

3.2 Energy Analysis Results

As inlet flow velocity increases, thermal energy efficiency decreases, as shown in Fig. (6). Figure (7) shows that at the lowest inlet velocity, the highest outlet temperatures are 328K for Alumina/water, 336.8K for Ag/water, 329K for MgO-MWCNT/water, and 330K for CuO-MWCNT/water. As flow

velocity increases, the gap between inlet and outlet temperatures narrows and trends toward zero. Figure (8) illustrates the variations in absorber plate temperature with varying flow speeds. At 0.24 m/s, the plate temperatures recorded were with temperatures of 321K for Alumina/water, 318K for Ag/water, 323K for MgO-MWCNT/water, and 322.36K for CuO-MWCNT/water.

As depicted in Fig. (6), Overall efficiency is determined by adding the electrical and thermal efficiencies of the module. At 0.24 m/s, the electrical efficiency reached 10.60% for Alumina/water, 10.8% for Ag/water, 10.5% for MgO-MWCNT/water, and 10.55% for CuO-MWCNT/water. The highest value was achieved using Ag/water. Accordingly, the PEEI (Percentage Electrical Efficiency Increase) for Ag/water was 14.2%. The MPEEI (Maximum Percentage of Electrical Efficiency Increase) calculated using pure water as the reference fluid was 3.61% for Alumina/water, 4.7% for Ag/water, 3.5% for MgO-MWCNT/water, and 3.37% for CuO-MWCNT/water. These values were calculated using Eqs. (12) and (13) (Khanjari et al., 2016). At 0.24 m/s, the overall efficiency was 90.12% for CuO-MWCNT/water, 82.7% for MgO-MWCNT/water, 69% for Ag/water, and 70% for Alumina/water.

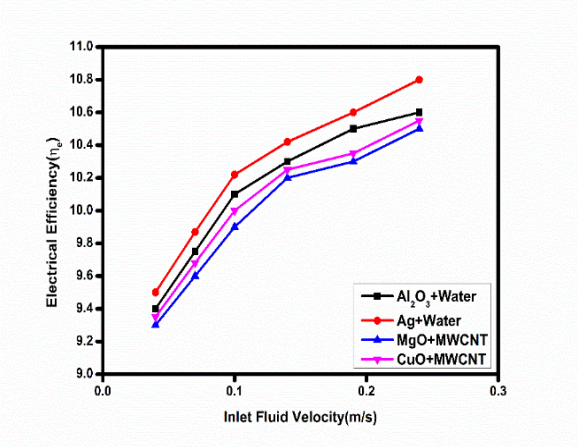

(a) Electrical efficiency vs Inlet Fluid Velocity

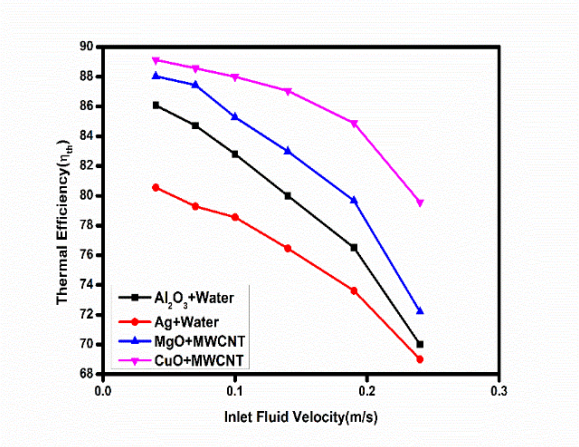

(b) Thermal Efficiency vs Inlet Flow Velocity

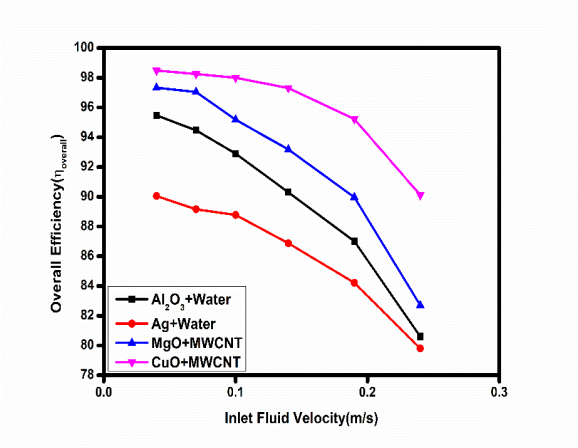

(c) Overall Efficiency vs Inlet Fluid velocity

Fig 6. Energy efficiency parameter fluctuation regarding inlet flow velocity

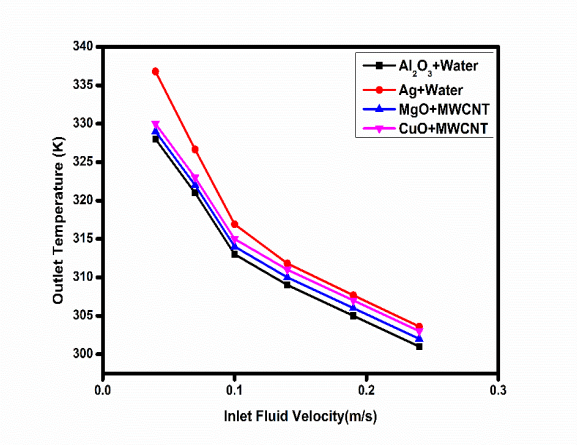

Fig 7. Outlet temperature regarding the inlet fluid velocity

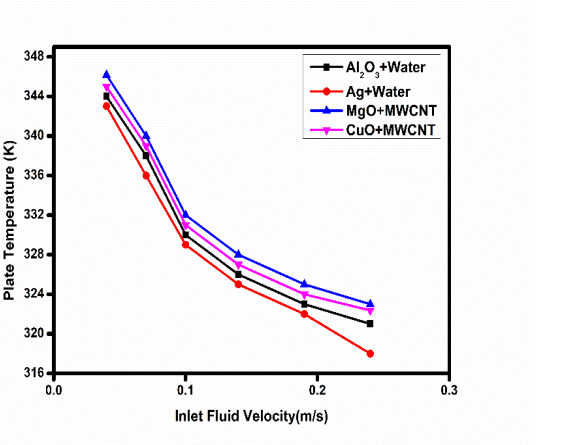

Fig 8. Plate-absorber temperature regarding the inlet fluid velocity

3.3 Exergy Analysis Results

Figure (10) presents the exergy efficiency of the photovoltaic thermal system as a function of inlet flow velocity, evaluated based on 2nd law of thermodynamics. The highest exergy efficiency observed in this study is 14.5% which is significantly lower than the overall energy efficiency values. Because electricity is considered useful work, the electrical exergy values in this study exceed the thermal exergy values. The total exergy efficiency is influenced by factors such as solar radiation exergy, ambient and absorber temperatures, packing factor, and both electrical and thermal efficiencies. A decreasing trend in exergy efficiency is observed with increasing flow speeds. At 0.24 m/s, the exergy efficiencies of the nanofluids were recorded as 11.8% for alumina/water, 12.2% for Ag/water, 11.2% for MgO-MWCNT/water, and 11.4% for CuO-MWCNT/water. Among these, Ag/water outperforms the other nanofluids because of its enhanced ability to conduct and transfer heat.

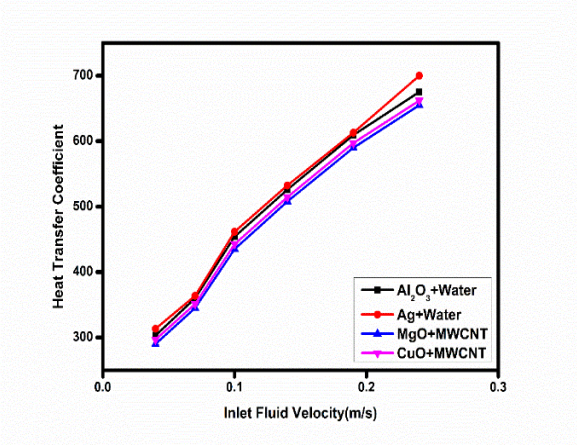

Fig 9. Heat transfer coefficient vs the inlet fluid velocity

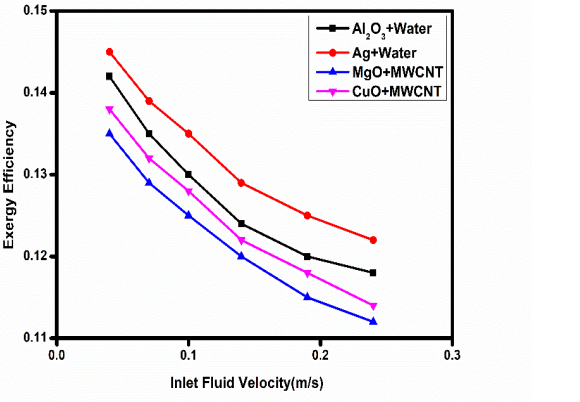

Fig 10. Exergy efficiency vs the inlet fluid velocity

4. DISCUSSION

4.1 Energy Efficiency Implications

The circulation of nanofluids behind a photovoltaic panel serves a dual function of cooling the cells and enhancing electrical output. Raising the nanofluid's inlet velocity decreases the absorber's surface

temperature, thereby improving electrical output. Reduction in thermal stress helps maintain lower operating temperatures and minimizes resistive losses. While Ag/water showed the highest electrical efficiency, the CuO-MWCNT/water nanofluid achieved the best overall energy efficiency. This is attributed to synergistic effects between CuO and MWCNT particles, which enhanced uniform heat distribution across the system, improving both thermal and total energy efficiency. At lower inlet velocities, the nanofluids flow through the channel for an extended period, resulting in higher outlet temperatures due to prolonged heat exchange. Conversely, higher inlet velocities increase the fluid's mass flow, thereby improving the total heat extraction from the PV panel. Figure (9) illustrates how the heat transfer coefficient varies with the flow speeds. As inlet flow velocity increases, the temperature gradient between the fluid inside the tubes and the collector rises, ultimately improving the heat transfer coefficient. However, if fluid temperature rises too much, the reduced thermal gradient with the PV panel further limits heat transfer. Additionally, as depicted in Fig. (9), the Ag-water nanofluid outperforms other mono and hybrid nanofluids in terms of heat transfer coefficients.

4.2 Exergy Efficiency Implications

The energy per unit flow decreases as the mass flow rate rises, indicating that higher flow rates do not necessarily enhance thermal performance in terms of useful energy output. This points to a key exergy principle that not all transferred energy is equally effective. While electrical efficiency improves with increased velocity, the associated rise in irreversibility reduces thermal exergy efficiency. At high inlet flow velocities, the minimal thermal variation between the inlet and outlet leads to reduced available work, making the system less suitable for thermal energy recovery in such cases. As evident in Fig. (10), Ag/water nanofluid demonstrates the highest exergy efficiency due to its superior thermal conductivity and reduced entropy generation, in contrast to the other nanofluids.

4.3 The Simulation Model's Temperature Contour

Figures (11) and (12) illustrate how temperature is distributed across the absorber surface and outlet for Ag/water nanofluids at 0.064 m/s inlet velocity. The contour results help visualize how the cold fluid in the tubes influences thermal behaviour within the nanofluid and across the absorber surface. Temperature elevation is noticeable along the paths from the inlet to the outlet and from the tube center to the wall. Notably, excessive temperature is observed at the peripheral regions of the absorber surface, attributed to the absence of tube cooling effects in this region. With each consecutive tube's inlet rotated by 180°, the flow distribution becomes more balanced, resulting in more uniform heat transfer across the absorber plate. The emergence of red spots between the two tubes indicates the absence of nanofluid cooling effects at those locations. Therefore, increasing the number of tubes would yield even better results.

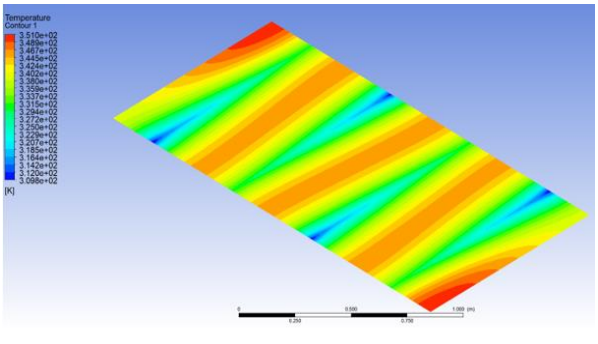

Fig 11. Absorber plate temperature distribution

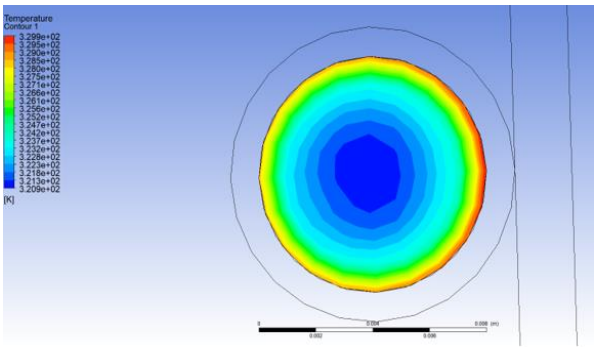

Fig 12. Fluid outlet temperature distribution

5. CONCLUSION

This study numerically investigated the efficiency and heat transfer of a PVT system using different nanofluids such as Ag/water, Al_2O_3/water, MgO-MWCNT/water, and CuO-MWCNT/water. It explored the influence of inlet fluid velocity under constant nanoparticle concentration on the energy and exergy efficiency. This investigation suggests that

- Nanoparticles enhance thermal conductivity and improve both energy and exergy efficiency.
- Higher inlet velocity improves electrical efficiency but reduces thermal and exergy performance.
- At 0.24 m/s, CuO-MWCNT/water achieved the best overall efficiency, while Ag/water achieved the highest electrical and exergy efficiency.

The analysis shows that exergy efficiency remains relatively low due to the poor heat quality compared to the high-grade electrical output. Nonetheless, the study confirms the potential of using mono and hybrid nanofluids for rear-side solar panel cooling to enhance overall performance. Ag/water nanofluid is recommended as a cost-effective cooling solution for the current PVT configuration. Future research should prioritize investigating the cooling capabilities of composite and homogeneous nanofluids, as well as internal turbulence enhancers like twisted tape inserts, helical tape inserts, and ball turbulators to improve PVT heat transfer.

NOMENCLATURE

A	Area/Packing factor	amb	Ambient
C_P	Specific heat	s	Sun
G	Solar irradiation	k	Thermal conductivity
P	Pressure	$\dot{E}_x$	Exergy
S	Radiation absorbed	n	Number of values
T	Temperature	RMSE	Root Mean Square Error
V	Volume		
g	Gravitational acceleration		
q	Heat flux		
v	Velocity		
$\dot{m}$	Mass flow rate		
Subscript		Greek symbols	
f	Base fluid	π	Pi number
nf	Nanofluid	β	Temperature coefficient
p	Nanoparticle	μ	Viscosity
in	Inlet	φ	Volume fraction
out	Outlet	η	Efficiency
NP	Nanoparticle	ρ	Density
T	Whole	II	2nd Law efficiency of Thermodynamics
g	Glass cover	α	Thermal diffusivity
r	Reference		
c	Cell/Cross-section		
e	Electrical		
th	Thermal		
amb	Ambient		

REFERENCES

Corbin, C. D., & Zhai, Z. J. (2010). Experimental and numerical investigation on thermal and electrical performance of a building integrated photovoltaic-thermal collector system. Energy and Buildings, 42(1), 76–82. https://doi.org/10.1016/j.enbuild.2009.07.013.

Davarnejad, R., & Jamshidzadeh, M. (2015). CFD modeling of heat transfer performance of MgO-water nanofluid under turbulent flow. Engineering Science and Technology, an International Journal, 18(4), 536–542. https://doi.org/10.1016/j.jestch.2015.03.011.

Drew, D. A., & Passman, S. L. (1999). Theory of multicomponent fluids. Applied Mathematical Sciences, 135. 1st ed. Springer New York, NY. https://doi.org/10.1007/b97678.

Ebaid, M. S. Y., Ghrair, A. M., & Al-Busoul, M. (2018). Experimental investigation of cooling photovoltaic (PV) panels using (TiO2) nanofluid in water-polyethylene glycol mixture and (Al2O3) nanofluid in water-cetyltrimethylammonium bromide mixture. Energy Conversion and Management, 155, 324–343. https://doi.org/10.1016/j.enconman.2017.10.074.

Hamdan, M., & Kardasi, K. (2017). Improvement of photovoltaic panel efficiency using nanofluid. The International Journal of Thermal & Environmental Engineering, 14(2), 143–151. https://doi.org/10.5383/ijtee.14.02.008.

Huminic, G., & Huminic, A. (2020). Entropy generation of nanofluid and hybrid nanofluid flow in thermal systems: A review. Journal of Molecular Liquids, 302, 112533. https://doi.org/10.1016/j.molliq.2020.112533.

Hussein, H., Numan, A., & Abdulmunem, A. (2017). An experimental investigation on the performance enhancement of photovoltaic/thermal panel using a tracking system and nanofluid (Al_2O_3). Engineering and Technology Journal, 35(5A), 493–508. https://doi.org/10.30684/etj.35.5A.9.

Hussien, H. A., Hasanuzzaman, M., Noman, A. H., & Abdulmunem, A. R. (2014). Enhance photovoltaic/thermal system performance by using nanofluid. 3rd IET International Conference on Clean Energy and Technology (CEAT) 2014, Kuching, 1–5. https://doi.org/10.1049/cp.2014.1515.

Ibrahim, A., Ramadan, M. R., Khallaf, A. E. M., & Abdulhamid, M. (2023). A comprehensive study for Al_2O_3 nanofluid cooling effect on the electrical and thermal properties of polycrystalline solar panels in outdoor conditions. Environmental Science and Pollution Research, 30(49), 106838–106859. https://doi.org/10.1007/s11356-023-25928-3.

Kell, G. S. (1975). Density, thermal expansivity, and compressibility of liquid water from 0 °C to 150 °C: Correlations and tables for atmospheric pressure and saturation reviewed and expressed on 1968 temperature scale. Journal of Chemical & Engineering Data, 20(1), 97–105. https://doi.org/10.1021/je60064a005.

Khanjari, Y., Pourfayaz, F., & Kasaeian, A. B. (2016). Numerical investigation on using of nanofluid in a water-cooled photovoltaic thermal system. Energy Conversion and Management, 122, 263–278. https://doi.org/10.1016/j.enconman.2016.05.083.

Kozak, T., Maranda, W., Napieralski, A., De Mey, G., & De Vos, A. (2009). Influence of ambient temperature on the amount of electric energy produced by solar modules. 2009 MIXDES–16th International Conference on Mixed Design of Integrated Circuits & Systems, Lodz, Poland, 351–354. https://ieeexplore.ieee.org/document/5289580.

Menter, F. R. (1993). Zonal two equation k-ω turbulence models for aerodynamic flows. 23rd Fluid Dynamics, Plasmadynamics, and Lasers Conference, Orlando, FL. American Institute of Aeronautics and Astronautics, 1993-2906. https://doi.org/10.2514/6.1993-2906.

Muneeshwaran, M., Srinivasan, G., Muthukumar, P., & Wang, C. C. (2021). Role of hybrid-nanofluid in heat transfer enhancement – A review. International Communications in Heat and Mass Transfer, 125. https://doi.org/10.1016/j.icheatmasstransfer.2021.105341.

Murtadha, T. K., & Hussein, A. A. (2022). Optimization the performance of photovoltaic panels using aluminum-oxide nanofluid as cooling fluid at different concentrations and one-pass flow system. Results in Engineering, 15. https://doi.org/10.1016/j.rineng.2022.100541.

Saffarian, M. R., Moravej, M., & Doranehgard, M. H. (2020). Heat transfer enhancement in a flat plate solar collector with different flow path shapes using nanofluid. Renewable Energy, 146, 2316–2329. https://doi.org/10.1016/j.renene.2019.08.081.

Sathyamurthy, R., Kabeel, A. E., Chamkha, A., Karthick, A., Muthu Manokar, A., & Sumithra, M. G. (2021). Experimental investigation on cooling the photovoltaic panel using hybrid nanofluids. Applied Nanoscience (Switzerland), 11(2), 363–374. https://doi.org/10.1007/s13204-020-01598-2.

Selmi, M., Al-Khawaja, M. J., & Marafia, A. (2008). Validation of CFD simulation for flat plate solar energy collector. Renewable Energy, 33(3), 383–387. https://doi.org/10.1016/j.renene.2007.02.003.

Shang, D.-Y. (2012). Free convection film flows and heat transfer. Heat and Mass Transfer (HMT). 2nd ed. Springer Berlin, Heidelberg. https://doi.org/10.1007/978-3-642-28983-5.

Tian, M. W., Khetib, Y., Yan, S. R., Rawa, M., Sharifpur, M., Cheraghian, G., & Melaibari, A. A. (2021). Energy, exergy and economics study of a solar/thermal panel cooled by nanofluid. Case Studies in Thermal Engineering, 28. https://doi.org/10.1016/j.csite.2021.101481.

Usama Siddiqui, M., Arif, A. F. M., Kelley, L., & Dubowsky, S. (2012). Three-dimensional thermal modeling of a photovoltaic module under varying conditions. Solar Energy, 86(9), 2620–2631. https://doi.org/10.1016/j.solener.2012.05.034.

Wu, S. Y., Guo, F. H., & Xiao, L. (2014). A Review on the Methodology for Calculating Heat and Exergy Losses of a Conventional Solar PV/T System. International Journal of Green Energy, 12(4), 379–397. https://doi.org/10.1080/15435075.2013.840833.

Xu, Z., & Kleinstreuer, C. (2014). Concentration photovoltaic-thermal energy co-generation system using nanofluids for cooling and heating. Energy Conversion and Management, 87, 504–512. https://doi.org/10.1016/j.enconman.2014.07.047.

Xuan, Y., & Roetzel, W. (2000). Conceptions for heat transfer correlation of nanofluids. International Journal of Heat and Mass Transfer, 43(19), 3701–3707. https://doi.org/10.1016/S0017-9310(99)00369-5.

Yu, W., & Choi, S. U. S. (2003). The role of interfacial layers in the enhanced thermal conductivity of nanofluids: A renovated Maxwell model. Journal of Nanoparticle Research, 5, 167–171. https://doi.org/10.1023/A:1024438603801.